ACS MEASUREMENT SCIENCE Au
AN OPEN ACCESS JOURNAL OF THE AMERICAN CHEMICAL SOCIETY

pubs.acs.org/measureau
Article

Novel Separation Media with Metal Oxide Nanostructures for Capillary Electrochromatography

Katsuya Nakano, Ryoma Kamei, Eisuke Kanao, Takuro Hosomi, Sayaka Konishi Yamada, Yasushi Ishihama, Takeshi Yanagida, and Takuya Kubo*

Cite This: ACS Meas. Sci. Au 2025, 5, 199–207
Read Online

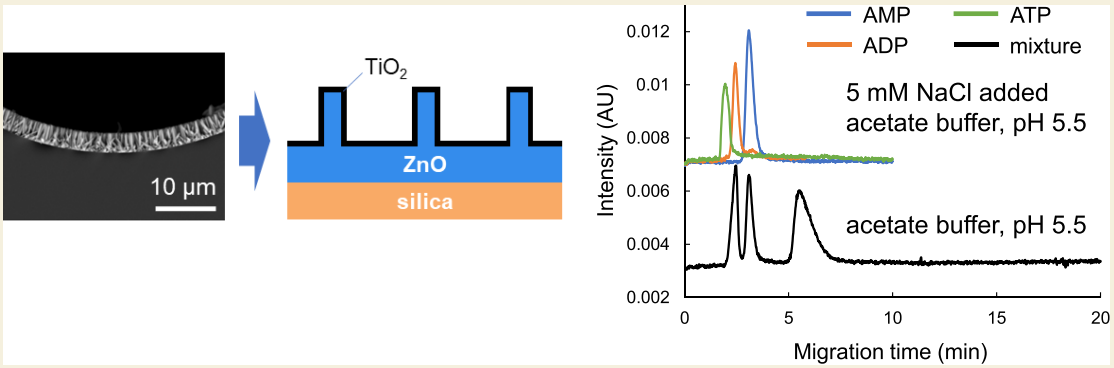

ABSTRACT: Zinc oxide nanowires (ZnO nanowire, ZnO NWs) are nanostructures that have drawn attention as separation media for efficient biomolecules because of high biological compatibility and low cost. Development of the capillary column (ZnO column) using a ZnO NW to an inner wall has been reported, although there are only a few studies about molecular recognition of a ZnO NW regardless of numerous studies reporting ZnO NWs. In our previous studies, we conducted fundamental research to elucidate molecular recognition of ZnO NW and develop a novel liquid phase separation field. Consequently, we achieved baseline separation of mixed adenosine phosphate analytes using a phosphate buffer in the mobile phase. In this study, to improve the low resistance of ZnO NW toward a solvent, we covered a surface of ZnO NW with titanium oxide (TiO_2) thin layers using atomic layer deposition. As a result, the column (TiO_2 NW column) showed high affinity toward acidic compounds like the ZnO column, strongly interacting with especially phosphate groups. Resistance of ZnO NW to a weak acidic buffer solution was then dramatically improved. This is because multipoint electrostatic interaction between the phosphate groups and the NW surface occurred. Next, we conducted capillary electrochromatography to examine the possibility for application of separation analysis. The elution order of the phosphorylated compound was successfully controlled by the migration solution containing aqueous acetonitrile with weak acids.

KEYWORDS: *ZnO nanowire, TiO_2, atomic layer deposition, acidic resistance, capillary electrochromatography*

1. INTRODUCTION

Metal oxides are known for thermally and chemically stable even under harsh conditions, and a number of application studies have been implemented because of various features of the metal oxides, such as ferroelectricity, ferromagnetism, metal−insulator transition, and memristors.[1−7] Notably, regarding metal oxide nanostructures, synthesis of different sorts of structures, such as nanosheets,[8] nanorods,[9] and nanoparticles,[10] has been reported since self-assembly was developed in the late 20th century. Nanostructures involve a large superficial area, high homogeneity, and crystalline nature, and anisotropy so that they can be the best candidates for new technological innovation in the fields of molecular recognition and detection.[11−13]

Among these metal oxide nanostructures, nanowires (NWs), a stick of nanostructures with a high aspect ratio, involve unique properties such as large specific surface area and high stability to high temperature. More studies about NW have been thus conducted lately, as bulk materials do not have these features. NWs consisting of ZnO, especially, have drawn much attention from an industrial point of view due to a simple synthesis process and efficient biological compatibility and biodegradability.[14] Development of a biorelated analysis based on unique interaction between ZnO NWs and biomolecules is one of the examples, and ZnO NWs are utilized in various devices, such as a sensor that detects immune globulin with high sensitivity and

Received: November 24, 2024
Revised: January 27, 2025
Accepted: January 29, 2025
Published: February 16, 2025

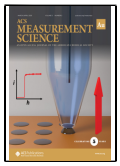

https://doi.org/10.1021/acsmeasuresciau.4c00089
ACS Meas. Sci. Au 2025, 5, 199−207

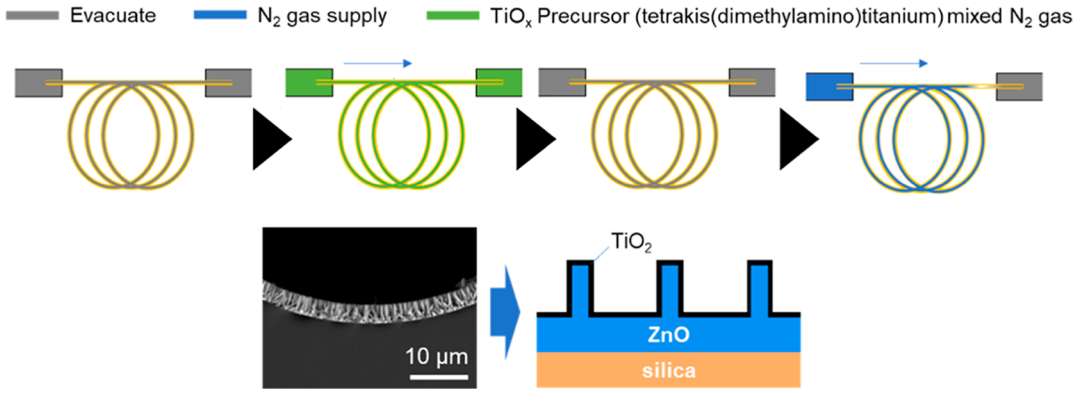

Figure 1. Use of TiO_2 for the ZnO column using ALD.

selectivity[15] and microfluidic devices that detect extracellular vesicle in urine.[16] While a number of application examples have been reported, there are few specific studies of ZnO NW molecular recognition. Examining ZnO NW molecular recognition may greatly contribute to developing a new perception for designing an efficient biomolecule detecting device.

In our previous studies, we have achieved the homogeneous growth of ZnO NWs with an aspect ratio of over 10,000 in a microtube, a length of 1 m, (ZnO column) by "flow assisted method" that is a synthesis technique using self-assembly.[17] When the micro tube was applied as a liquid chromatography (LC) column, Zn^{2+} atom with a Lewis acid group interacted, and specific retention of some analytes was observed. ZnO NW molecular recognition may thus be found by evaluating the retention characteristics of the ZnO column. Additionally, we elucidated ZnO NW molecular recognition in aqueous solvents with LC using different analytes, confirming high affinity to an acidity function and especially to a phosphate group. Also, we observed selective molecular recognition to the number of phosphate groups in nucleotides using the (100) face on the ZnO NW surface. Consequently, complete separation of adenosine oxidant (AMP, ADP, ATP) was achieved by optimizing the aqueous mobile phase and length of a column.[18] However, phosphate included in a migration buffer peeled off NWs from the inner walls of the column, which diminished retention capacity. To apply the ZnO column for separation analysis, resistance toward a NW solvent thus needs to be increased. To improve resistance, we prepared a NW column with various metal oxides, fabricating a novel ZnO column with titanic oxide (TiO_2). TiO_2 involves stronger resistance toward high salty and acidity compared to ZnO. TiO_2 has been frequently applied to the concentration technique for biologically relevant substances such as phosphorylated peptides and exosomes as Lewis acids on a Ti atom surface are high.[19−21] Therefore, the use of TiO_2 to ZnO NWs may be optimal for the application of a biomolecule analysis. Given this, we covered the ZnO NW surface with TiO_2 thin layers by using atomic layer deposition (ALD). The previous study reported that a limited surface area was covered with various metal oxide thin layers using ALD. This technique enables us to cover nanostructure surfaces inside of a capillary with metal oxide thin layers, and accordingly, a novel analytical column can be developed.[22]

In this study, we evaluated resistance toward solvents and retention characteristics for a novel ZnO column (TiO_2 NW column) and a ZnO seed layer column, both of them were covered with TiO_2 thin layers using ALD, then evaluating properties and utilities of the columns as an analytical column. Next, according to properties of resistance toward solvents of the ZnO column with TiO_2 and high affinity to the phosphate group, capillary electrochromatography (CEC) using adenosine phosphate was conducted to seek the possibility for applications of biomolecule analyses. A flow rate and direction of electroosmotic flow (EOF) are opted depending on zeta potential and salt concentration, which are largely affected by pH and ionic strength of migration solution. Since the isoelectric point of TiO_2 is 6−7,[23] we expected that a flow rate of EOF can be controlled by changing a solvent to weak acidity, neutrality, and basicity. Conditions for separation of adenosine phosphates were considered by altering pH buffer solutions using the TiO_2 column having a strong acidic resistance. We also observed how migration behavior changed after adding acetonitrile to lower polarity of migration solutions.

2. EXPERIMENTAL SECTION

2.1. Preparation and Evaluation of a TiO_2-Modified Capillary Column

The ZnO NW column and the TiO_2-deposited NW column (TiO_2 NW column) were prepared by a similar method to our previous study.[22] The schematic procedure is shown in Figure 1. To evaluate resistance toward solvents, LC measurements and SEM observations were conducted using the NW column before and after solvents were flowed.

LC was implemented under the conditions below, and the surface of the column was observed with SEM. Solvents were flowed to the ZnO column and the TiO_2 column by using the syringe pump (1 μL/min). Column internal was washed by flowing water using the syringe pump (3 μL/min, 20 min). LC and SEM observations were implemented under the same conditions as above, and the results before and after solvents were flowed were compared.

2.2. Nano LC Evaluations

The instruments for the nano LC evaluations are summarized in the Supporting Information. The detailed LC conditions for the evaluation of resistance toward solvents and retention selectivity are also indicated in the Supporting Information.

2.3. CEC and capillary zone electrophoresis (CZE) Measurements

To consider separation conditions of adenosine phosphate using CEC, CZE was implemented under the condition that weak acidic buffers inhibiting EOF were applied as migration solutions. The measurement to accelerate interaction with a stationary phase was implemented by adding acetonitrile to the

https://doi.org/10.1021/acsmeasuresciau.4c00089
ACS Meas. Sci. Au 2025, 5, 199−207

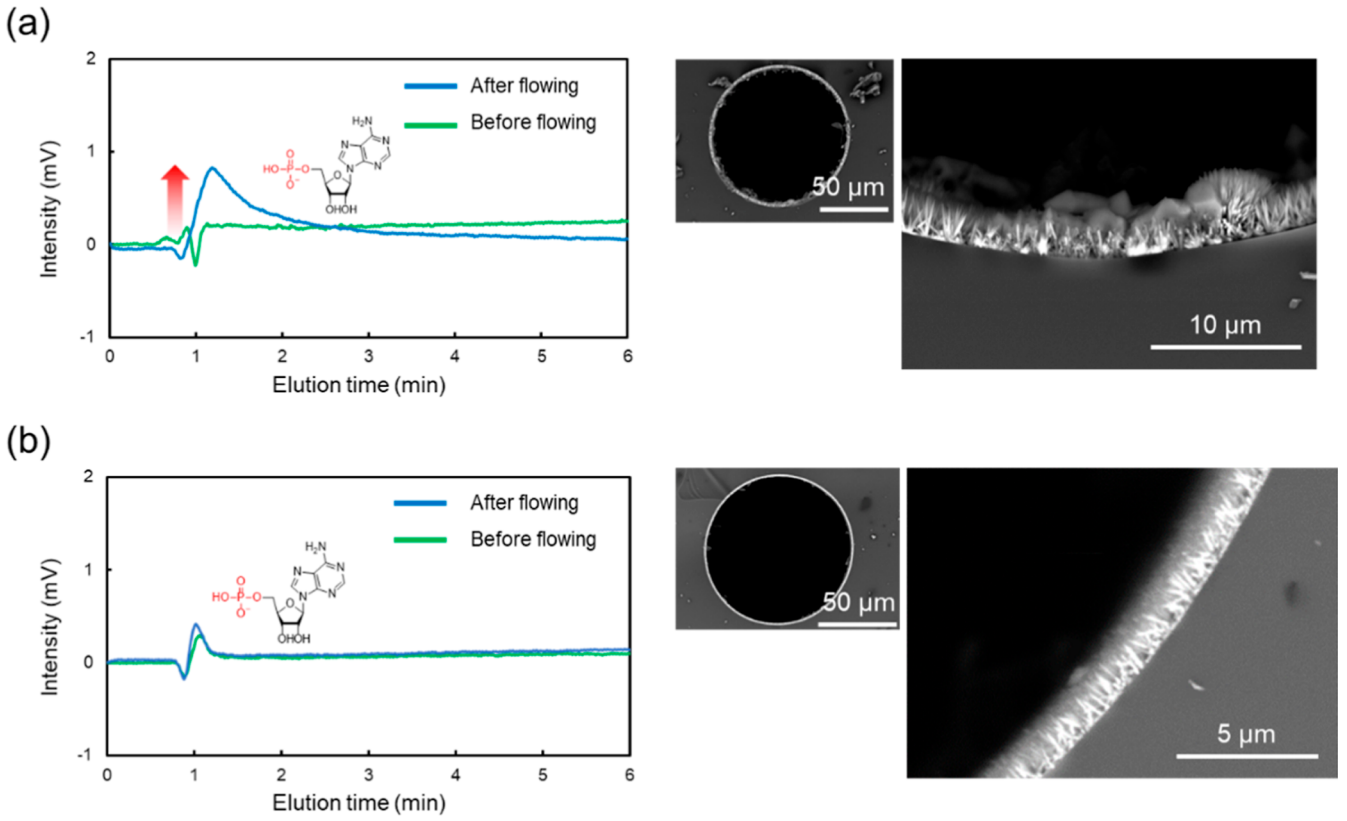

Figure 2. Result of evaluation of resistance toward solutions for the (a) ZnO NW column and (b) TiO_2 NW column. Chromatograms of AMP before and after flowing 1 mM acetate buffer as a solvent, and SEM images.

migration solution, where adenosine phosphate is completely separated. The detailed conditions are summarized in the Supporting Information.

3. RESULTS AND DISCUSSION

3.1. Evaluation of Resistance of TiO_2 NW Solvents

Figure 2 shows evaluation of resistance using 1 mM acetate buffer as a solvent. Before the buffer was flowed, AMP was adsorbed to each column. According to the result of LC measurements after the buffer was flowed, while recovery amounts of AMP decreased with the ZnO NW column, AMP was completely recovered with the TiO_2 NW column as the retention capacity was maintained. The figure also shows a cross section of the column before and after the buffer was flowed. NW structures were partly collapsed, and deposition occurred when the buffer was flowed to the ZnO NW column. However, NW was not collapsed, and its structures were maintained with the TiO_2 NW column. These results confirmed that the column resistance was improved using TiO_2.

According to the evaluation of resistance under the condition with lowered buffer pH, NW structures and retention capacity were maintained the same as Figure S1. It revealed strong resistance toward weak acetate salt and formate buffers.

3.2. Evaluation of Retention Characteristics of the TiO_2 NW Column

Figure S2 shows the results of LC for monosubstituted benzenes using water as a mobile phase and their peak area ratio toward the open tubular column. For comparison, the TiO_2-modified capillary (the TiO_2 column), which was prepared with a simple TiO_2 layer, was also evaluated. With the TiO_2 NW column, analytes were not retained and were not adsorbed, resulting in complete elution. On the contrary, with the TiO_2 column, the peak area ratio of benzyl amine involving an amino group slightly decreased. It might suggest high affinity toward the basic function of the TiO_2 column.

Additionally, we conducted another LC using acetonitrile as the mobile phase. The results shown in Figure 3 confirmed that benzyl amine was adsorbed with the TiO_2 NW column as well. Moreover, the peak area ratio with analytes involving the acidity function, such as benzenesulfonic acid, phenyl phosphate, and benzoic acid, dramatically decreased. It revealed high affinity toward the basicity and acidity function due to modification of TiO_2. The decrease in the peak area ratio demonstrated high affinity, especially toward the acidity function.

Similarly, Figure S3 shows the peak area ratio obtained from the measurement using a basic analyte. As a result of the measurement using the basic analyte with various acid dissociation constants, piperidine involving high basicity mostly adsorbed and did not elute. As basicity increased, the peak area ratio decreased, confirming strong interactions with analytes having high basicity. The significant increase in Lewis acidity on the NW surface treated with TiO_2 modification may have caused the outcome that noncovalent electron pairs of the nitrogen atom in the analyte having high basicity may be strongly attracted by the Ti^{4+} atom.

Figure 4 shows the result of LC using water/acetonitrile mixed solvents. A few analytes were retained more by adding 20% water in acetonitrile. In particular, phenyl phosphate involving a phosphate group was strongly retained. Then, the retention time of each composition, water/acetonitrile mixed solvents, was measured (Figure 4b). Accordingly, all analytes

https://doi.org/10.1021/acsmeasuresciau.4c00089
ACS Meas. Sci. Au 2025, 5, 199−207

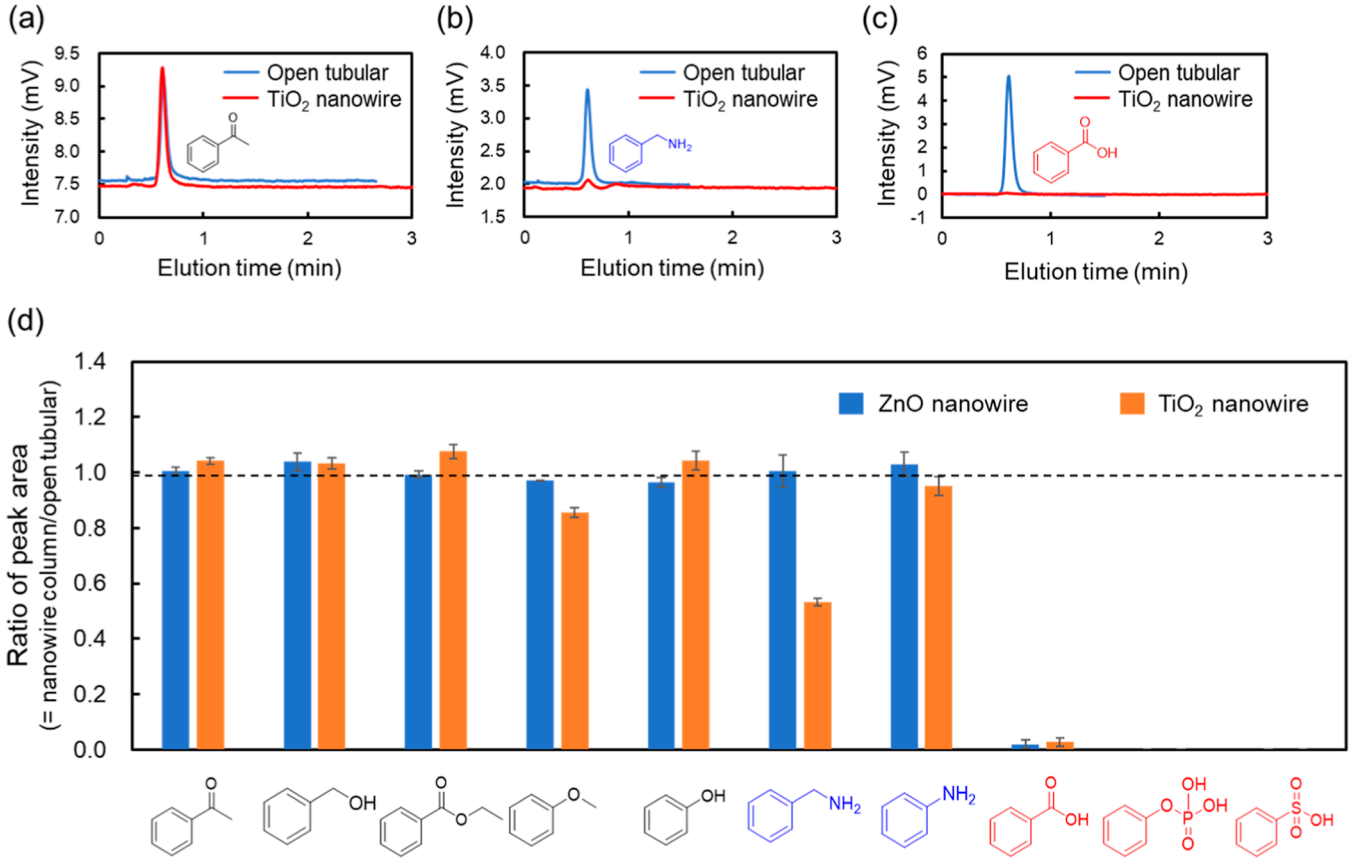

Figure 3. Chromatograms for (a) acetophenone, (b) benzylamine, (c) benzoic acid, and (d) the peak area ratio from the measurement of the ZnO NW column and the TiO_2 NW column. Column: the ZnO NW (27.0 cm × 100 μm I.D.), the TiO_2 NW (27.0 cm × 100 μm I.D.), open tubular column (27.0 cm × 100 μm I.D.); temperature, 25 °C; detection, UV (254, 260, 270 nm); mobile phase, acetonitrile; flow rate, 5000 nL/min; analytes: 100 ppm, 50 nL.

were not retained in the case of adding 50% water although the retention time of phenyl phosphate dramatically increased by reducing the rate of water to 20%. This result revealed that the TiO_2 NW column strongly interacted with phosphate groups, the same as the ZnO NW column.

To evaluate molecular recognition to the acidic analytes, the LC of organic acids having similar structures was implemented. When acetonitrile was applied as a mobile phase, trifluoroacetic acid with a low acid dissociation constant (pK_a −0[37]) adsorbed and did not elute. In contrast, acetic acid with a high acid dissociation constant (pK_a = 4.8[37]) was slightly retained, and complete elution was observed. According to these results, the range of acidity level of the analytes, that is, the magnitude of the acid dissociation constant, may affect the retention behavior of the TiO_2 NW column. Also, electrostatic interaction with the Ti atom on the surface may cause retention adsorption of the analyte.

The measurement results of the acidic analytes show that phenyl phosphate interacted most (Figure 4). However, considering the acid dissociation constant, this is not consistent with pK_a value becoming larger in order from benzenesulfonic acid (pK_a = −2.738), phenyl phosphate (pK_a = 1.7949) to benzoic acid (pK_a = 4.1440). This is because multipoint interaction between only the phosphate group and Ti atom on the NW surface occurred as the phosphate group involves a double negative charge and other phosphate groups involve a single negative charge. Thus, phosphate groups more strongly interacted than other functional groups, showing a high affinity.

3.3. LC Measurement Using Adenosine Phosphate

Figure 5a shows the result of the LC measurement with the TiO_2 NW column using adenosine phosphates. According to the measurement using water as a mobile phase, adenosine monophosphate (AMP) was eluted, and in contrast, adenosine diphosphate (ADP) and adenosine triphosphate (ATP) were adsorbed. The peak area ratios of each analyte with the TiO_2-coated column (the TiO_2 column) and the ZnO NW column to an open tubular column were then calculated (Figure 5b). The result showed that the recovery rate of the analytes was higher with AMP compared to ADP and ATP. Adenosine phosphates showed the same retention behavior compared to the result with the ZnO NW column.

3.4. CZE Measurement Using Adenosine Phosphates

Figure 6 shows the result of CZE for ATP using a TiO_2 NW column. ATP eluted by pressuring toward the detector under the condition applying voltage at −20 kV. Then, the measurement applied at 0.2 psi was implemented. Adenosine phosphates eluted in ascending order of the phosphate groups, and baseline separation using a TiO_2 NW column was achieved.

Next, to observe the migration behavior of adenosine phosphates, the effects of migration solution, applied voltage, and salt concentration were evaluated. Figure S4 shows the measurement result when the applied voltage was gradually changed. The migration time of only AMP increased along with the decrease in applied voltage. It is because EOF velocity increased along with the increase in applied voltage. EOF

https://doi.org/10.1021/acsmeasuresciau.4c00089
ACS Meas. Sci. Au 2025, 5, 199−207

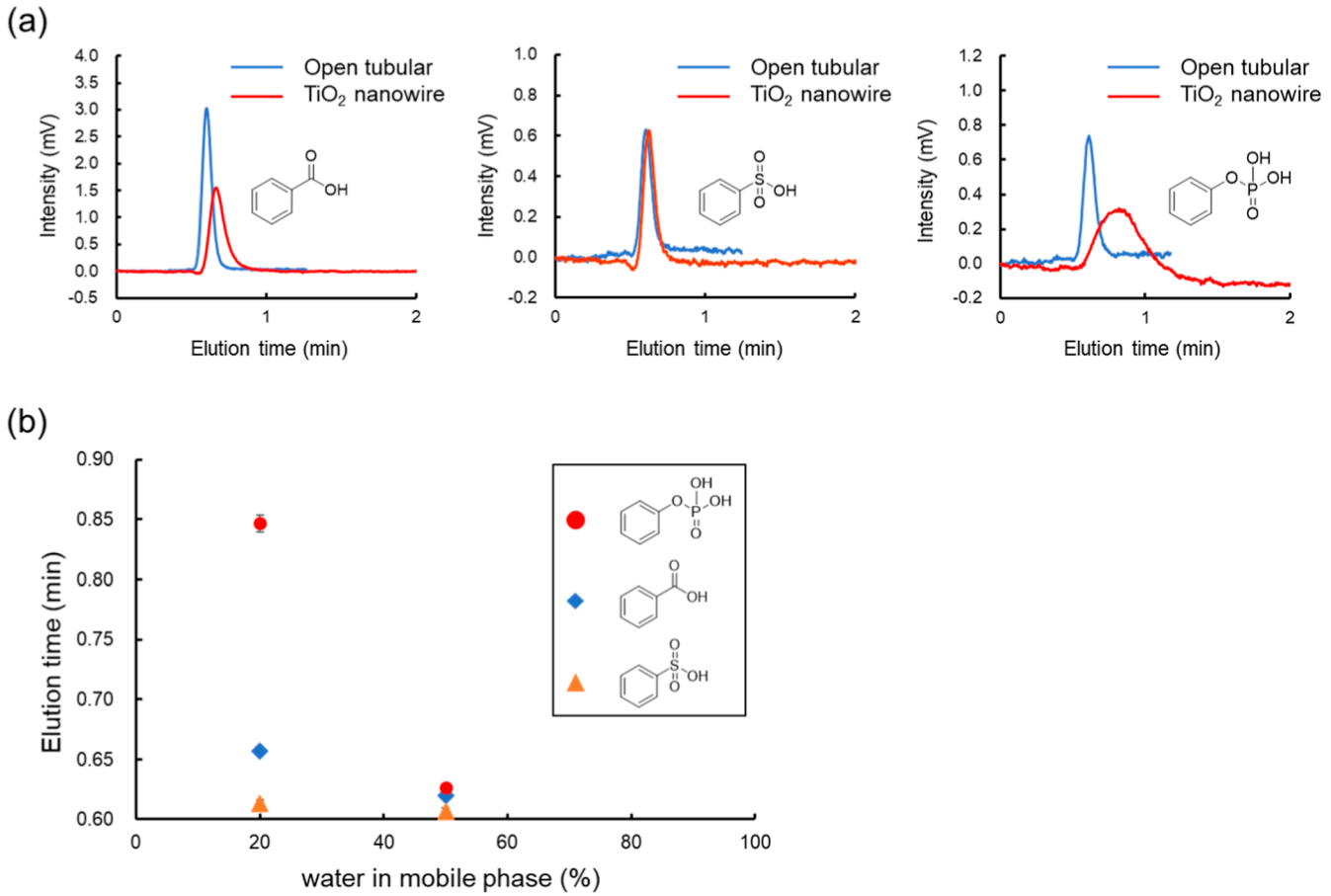

Figure 4. (a) Result of LC of acidic analytes with water/acetonitrile = 2/8 as a mobile phase. (b) Retention time of the analytes by each mobile phase composition. Column: the TiO_2 NW (27.0 cm × 100 μm I.D.), open tubular column (27.0 cm × 100 μm I.D.); temperature, 25 °C; detection, UV (254, 260, 270 nm); mobile phase, acetonitrile; flow rate, 5000 nL/min; analytes: 100 ppm, 50 nL.

oppositely flows toward the detector, and the velocity increased as voltage increased. Consequently, the migration time of AMP involving fewer phosphate groups, that is, involving larger electrophoretic mobility, increased.

Furthermore, we conducted measurements with various pH values in migration solution. Figure 7 shows the CZE results. The measurement with pH 4.5, 5.5 acetate buffer showed the shorter migration time of nucleotides and the improved peak shapes in the case of pH 5.5. It may be caused by the increase in the ratio of nucleotides negatively charging in the migration solution. Figure 7b shows the result of various electrolyte concentrations with added NaCl. The peak width and the migration time were changed by adding NaCl, and then the efficient peak separations due to a higher plate number were observed. Based on these results, the separation conditions of nucleotides can be further optimized by altering electrolyte concentration and pH in migration solution.

3.5. CEC Measurement Using Adenosine Phosphate

Figure 8 shows the measurement result of each nucleotide when acetonitrile was added. After acetonitrile was increased to 80% and electrolyte concentration was altered with NaCl, nucleotides eluted in ascending order of phosphate groups, which was the contrary result from CZE. To observe the difference of mobility with each migration solution, electrophoretic mobility of each analyte was then calculated using the migration time obtained from this result and the migration time of a neutral molecule (thiourea) (Figure 8b). Accordingly, electrophoretic mobility increased by adding acetonitrile. It is explained that acetonitrile suppressed electroosmotic flow more than the buffer alone. Electrophoretic mobility of nucleotide increased as well, and a magnitude relation of mobility changed as AMP > ADP > ATP to ATP > ADP > AMP. Electrostatic interaction between the analyte and titanium occurred by adding acetonitrile. The migration rate decreased because the analytes involving more phosphate groups led to a stronger interaction.

To improve peak shapes and achieve complete separation of the analytes, we optimized the measurement conditions. Electrolyte concentration was increased by adding NaCl in the migration solution to completely separate each peak of the analytes, and electroosmotic flow that oppositely flows toward the detector was increased. Figure 8c shows the measurement result with 30 mM NaCl. The increase in the migration time of each analyte was observed by adding NaCl. However, due to poor peak shapes, better conditions for separation analysis of the plate height should be considered.

4. CONCLUSIONS

We utilized TiO_2 for the ZnO NW column using ALD to improve its utility as a biomolecule analysis column. According to various evaluations of resistance to different solvents, retention capacity and the NW structures did not change with weak acetate salt and formate buffers even after flowing the buffers, and resistance was certainly improved. Furthermore, we evaluated retention characteristics using a TiO_2 NW column.

https://doi.org/10.1021/acsmeasuresciau.4c00089
ACS Meas. Sci. Au 2025, 5, 199−207

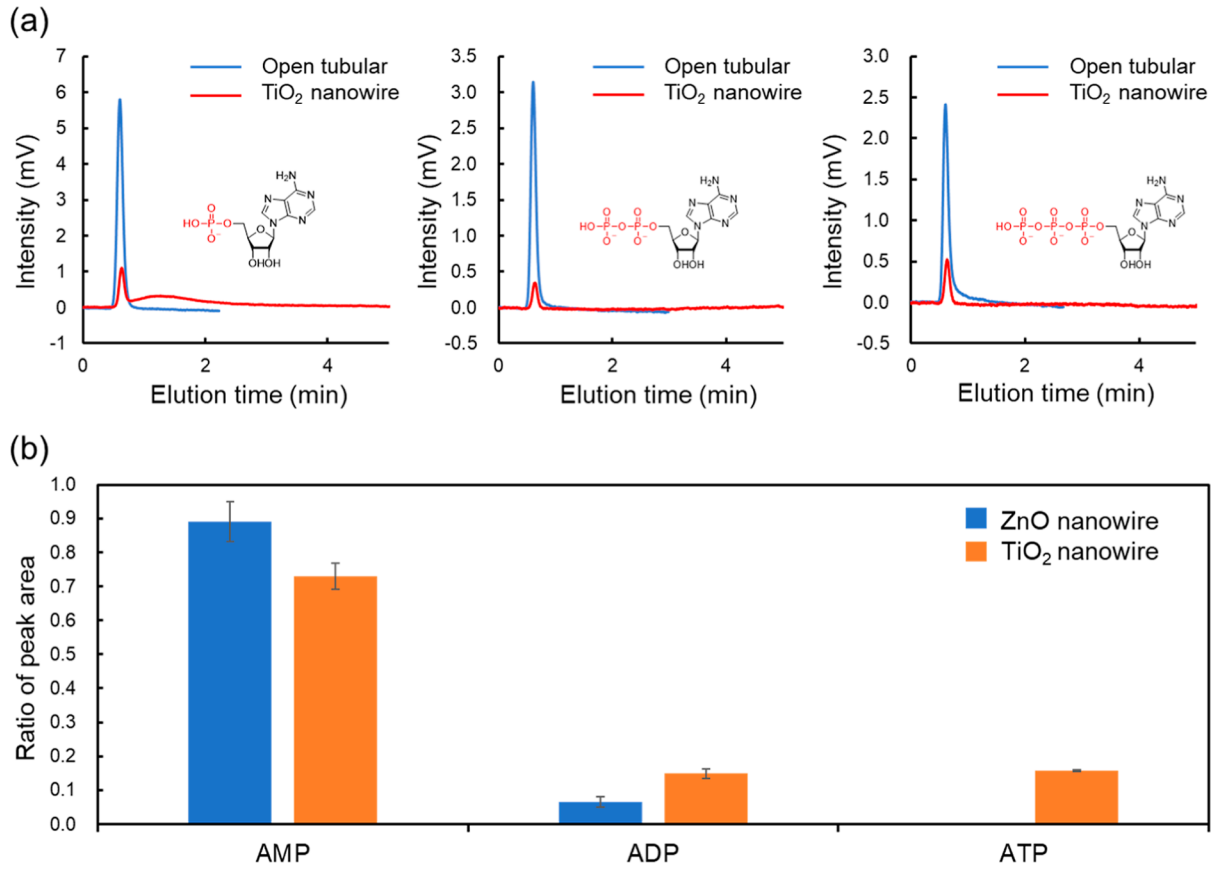

Figure 5. (a) Result of LC using adenosine phosphates. (b) Peak area ratio calculated from the measurement with the ZnO column and the TiO_2 NW column: the TiO_2 nanowire column (27.0 cm × 100 μm I.D.), open tubular column (27.0 cm × 100 μm I.D.); temperature, 25 °C; detection, UV (260 nm); mobile phase, water; flow rate, 5000 nL/min; analytes, AMP, ADP, ATP (100 ppm, 50 nL).

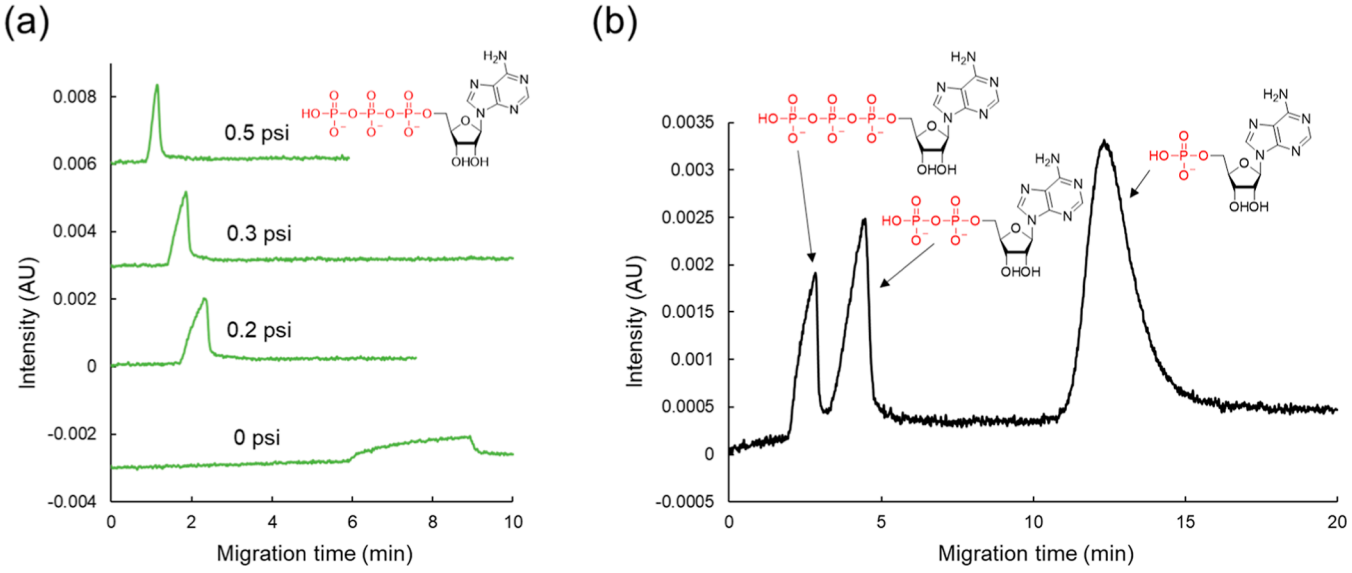

Figure 6. (a) CZE result of ATP at various pressures. (b) CZE result of adenosine phosphates at 0.2 psi Conditions: column: TiO_2 NW column (an effective length 20 cm, a length 30 cm); injection, 0.5 psi, 5s; detection, UV (254 nm); applied voltage, −20 kV; pressure, 0, 0.2, 0.3, 0.5 psi; migration solution, 1 mM acetate buffer (pH 4.5); analyte, ATP (100 ppm, 50 nL).

High affinity toward basicity and the phosphate group was then observed as benzyl amine involving a basic function and the analyte involving the acidity function was mostly adsorbed in the NW column. LC using various basic analytes showed that high basic analytes were adsorbed in the column. This is because TiO_2 modification increased Lewis acid on the NW surface, and the Ti^{4+} atom attracted noncovalent electron pairs in the basic analytes. As the result of the measurement using the organic acids, the magnitude of acid dissociation constant affected retention adsorption of analytes as the analytes with lower acid

https://doi.org/10.1021/acsmeasuresciau.4c00089
ACS Meas. Sci. Au 2025, 5, 199−207

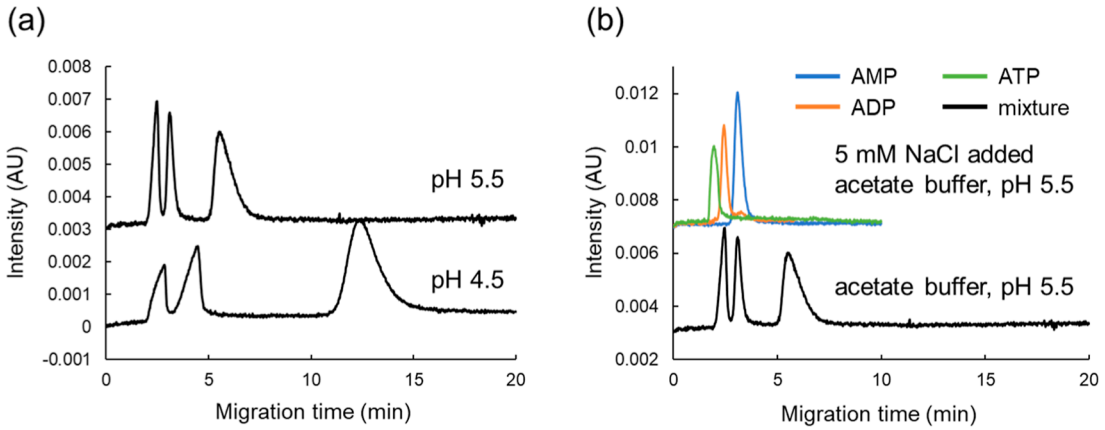

Figure 7. (a) pH in migration solution. (b) Measurement result with various salt concentrations in migration solution.

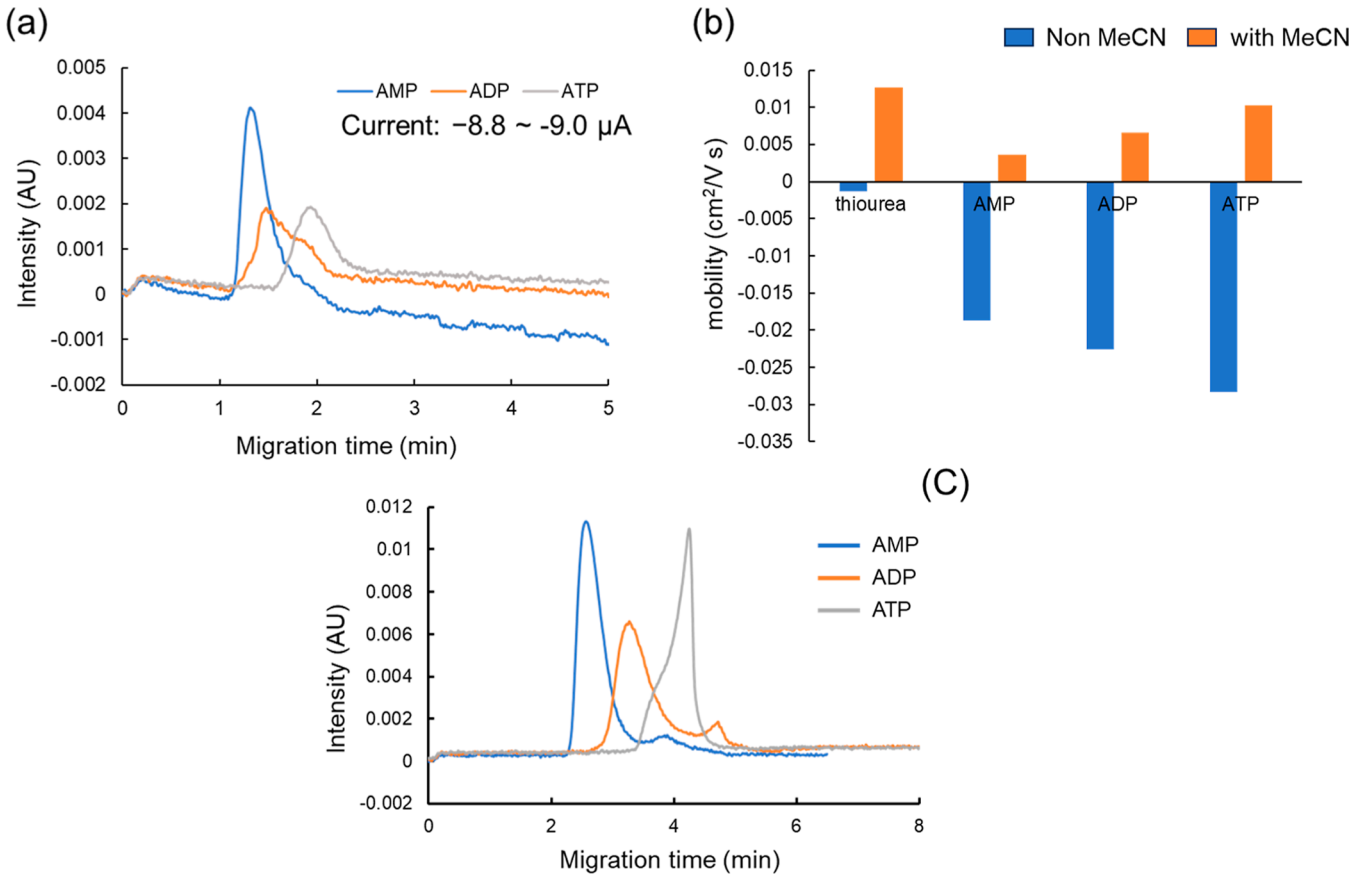

Figure 8. (a) CEC result with 10 mM NaCl. (b) Mobility of analytes under each measurement condition on (a). (c) Measurement result with 30 mN NaCl. Column: TiO_2 NW column (an effective length 20 cm, a length 30 cm), injection: 0.5 psi, 5 s; detection, UV (254 nm); migration solution, 10 mM NaCl + 1 mM acetate buffer (pH 5.5)/acetonitrile = 20/80, 30 mM NaCl + 1 mM acetate buffer (pH 5.5)/acetonitrile = 20/80; analytes, thiourea, AMP, ADP, ATP (100 ppm, 50 nL).

dissociation constant were adsorbed more. Multipoint interaction may cause affinity to the phosphate group due to a double negative charge.

Additionally, LC for the TiO_2 NW column showed that the recovery rate was higher with AMP compared with ADP and ATP using water as a mobile phase, and selectivity to the number of phosphate groups was confirmed the same as the ZnO NW column. This suggested that application for separation analysis of adenosine phosphate may be available. To implement an analysis of adenosine phosphate with a higher separation efficiency, we applied CE. Consequently, CZE using the TiO_2 NW column enabled complete separation of the adenosine phosphate mixture. As the separation improved by altering electrolyte concentration and pH in migration solution, separation conditions of nucleotides can be further optimized. Moreover, the analytes eluted in ascending order of the phosphate groups by adding acetonitrile in migration solution, showing the different result; the analytes eluted in descending order of the phosphate groups, from CZE measurement. Change of electrophoretic mobility magnitude of adenosine phosphate led to interaction between TiO_2 in the inner wall of the TiO_2 NW column and adenosine phosphates, resulting in late elution

https://doi.org/10.1021/acsmeasuresciau.4c00089
ACS Meas. Sci. Au 2025, 5, 199−207

of the analytes involving more phosphate groups. Therefore, these results suggested that the TiO_2 NW column can be effectively applied to CEC. In the future, applications of an NW column for biomolecule analyses by CEC and LC can be expanded.

■ ASSOCIATED CONTENT

Supporting Information

The Supporting Information is available free of charge at https://pubs.acs.org/doi/10.1021/acsmeasuresciau.4c00089.

Experimental including chemicals, instruments, nano-LC conditions, and CZE conditions, resistance evaluation of the TiO_2 NW column, chromatograms and peak area ratio from the result of LC measurement, peak area ratio from LC measurement using basic analytes, and CZE migration with the TiO_2 NW column (PDF)

■ AUTHOR INFORMATION

Corresponding Author

Takuya Kubo − *Graduate School of Engineering, Kyoto University, Kyoto 615-8510, Japan; Graduate School of Life and Environmental Science, Kyoto Prefectural University, Sakyo-ku, Kyoto 606-8522, Japan;* orcid.org/0000-0002-9274-3295; Phone: +81-75-703-5629; Email: tkubo@kpu.ac.jp

Authors

Katsuya Nakano − *Graduate School of Engineering, Kyoto University, Kyoto 615-8510, Japan*

Ryoma Kamei − *Seinan Indusutries, Co. LTD, Osaka 559-0011, Japan*

Eisuke Kanao − *Graduate School of Pharmaceutical Sciences, Kyoto University, Sakyo-ku, Kyoto 606-8501, Japan; National Institutes of Biomedical Innovation, Health and Nutrition, Ibaraki, Osaka 567-0085, Japan;* orcid.org/0000-0001-7268-1501

Takuro Hosomi − *Department of Applied Chemistry, Graduate School of Engineering, The University of Tokyo, Tokyo 113-8654, Japan;* orcid.org/0000-0002-5649-6696

Sayaka Konishi Yamada − *Graduate School of Life and Environmental Science, Kyoto Prefectural University, Sakyo-ku, Kyoto 606-8522, Japan*

Yasushi Ishihama − *Graduate School of Pharmaceutical Sciences, Kyoto University, Sakyo-ku, Kyoto 606-8501, Japan;* orcid.org/0000-0001-7714-203X

Takeshi Yanagida − *Department of Applied Chemistry, Graduate School of Engineering, The University of Tokyo, Tokyo 113-8654, Japan;* orcid.org/0000-0003-4837-5701

Complete contact information is available at: https://pubs.acs.org/10.1021/acsmeasuresciau.4c00089

Author Contributions

All authors contributed to and have given approval for the final version of the manuscript. CRediT: T. Kubo supervision, project administration, funding acquisition, conceptualization, methodology, writing-original draft, writing-review and editing; E. Kanao, T. Hosomi, Y. Ishihama, T. Yanagida conceptualization, data curation, formal analysis, K. Nakano data curation, investigation, methodology, S. K-Yamada writing-original draft, writing-review and editing. CRediT: **Katsuya Nakano** data curation; **Ryoma Kamei** data curation, formal analysis; **Eisuke Kanao** data curation, formal analysis, supervision, validation; **Takuro Hosomi** conceptualization, methodology, supervision; **Sayaka Konishi Yamada** writing - original draft, writing - review & editing; **Yasushi Ishihama** conceptualization, supervision, validation; **Takeshi Yanagida** conceptualization, methodology, supervision.

Notes

The authors declare no competing financial interest.

■ ACKNOWLEDGMENTS

This work was partly supported by JST, CREST grant nos. JPMJCR2332, JST A-STEP, JPMJTR214C, and the Environment Research and Technology Development Fund (JPMEERF20235003) of the Environmental Restoration and Conservation Agency of Japan.

■ REFERENCES

(1) Stengel, M.; Vanderbilt, D.; Spaldin, N. A. Enhancement of ferroelectricity at metal−oxide interfaces. *Nat. Mater.* **2009**, *8* (5), 392−397.

(2) Hwang, H. Y.; Iwasa, Y.; Kawasaki, M.; Keimer, B.; Nagaosa, N.; Tokura, Y. Emergent phenomena at oxide interfaces. *Nat. Mater.* **2012**, *11* (2), 103−113.

(3) Bristowe, N.; Varignon, J.; Fontaine, D.; Bousquet, E.; Ghosez, P. Ferromagnetism induced by entangled charge and orbital orderings in ferroelectric titanate perovskites. *Nat. Commun.* **2015**, *6* (1), 6677.

(4) Li, W.; Zhao, J.; Cao, L.; Hu, Z.; Huang, Q.; Wang, X.; Liu, Y.; Zhao, G.; Zhang, J.; Liu, Q.; et al. Superconductivity in a unique type of copper oxide. *Proc. Natl. Acad. Sci. U.S.A.* **2019**, *116* (25), 12156−12160.

(5) Zhang, S.; Vo, H.; Galli, G. Predicting the onset of metal−insulator transitions in transition metal oxides-a first step in designing neuromorphic devices. *Chem. Mater.* **2021**, *33* (9), 3187−3195.

(6) Braham, E. J.; Sellers, D.; Emmons, E.; Villarreal, R.; Asayesh-Ardakani, H.; Fleer, N. A.; Farley, K. E.; Shahbazian-Yassar, R.; Arroyave, R.; Shamberger, P. J.; et al. Modulating the hysteresis of an electronic transition: launching alternative transformation pathways in the metal−insulator transition of vanadium (IV) oxide. *Chem. Mater.* **2018**, *30* (1), 214−224.

(7) Wang, T.; Shi, Y.; Puglisi, F. M.; Chen, S.; Zhu, K.; Zuo, Y.; Li, X.; Jing, X.; Han, T.; Guo, B.; et al. Electroforming in metal-oxide memristive synapses. *ACS Appl. Mater. Interfaces* **2020**, *12* (10), 11806−11814.

(8) Xu, C.; Shi, S.; Sun, Y.; Chen, Y.; Kang, F. Ultrathin amorphous manganese dioxide nanosheets synthesized with controllable width. *Chem. Commun.* **2013**, *49* (66), 7331−7333.

(9) Hanske, C.; Hill, E. H.; Vila-Liarte, D.; González-Rubio, G.; Matricardi, C.; Mihi, A.; Liz-Marzán, L. M. Solvent-assisted self-assembly of gold nanorods into hierarchically organized plasmonic mesostructures. *ACS Appl. Mater. Interfaces* **2019**, *11* (12), 11763−11771.

(10) Das, S. K.; Bhunia, M. K.; Bhaumik, A. Self-assembled TiO 2 nanoparticles: mesoporosity, optical and catalytic properties. *Dalton Trans.* **2010**, *39* (18), 4382−4390.

(11) Hahn, Y.-B.; Ahmad, R.; Tripathy, N. Chemical and biological sensors based on metal oxide nanostructures. *Chem. Commun.* **2012**, *48* (84), 10369−10385.

(12) Li, Z.; Li, H.; Wu, Z.; Wang, M.; Luo, J.; Torun, H.; Hu, P.; Yang, C.; Grundmann, M.; Liu, X.; et al. Advances in designs and mechanisms of semiconducting metal oxide nanostructures for high-precision gas sensors operated at room temperature. *Mater. Horiz.* **2019**, *6* (3), 470−506.

(13) Limo, M. J.; Sola-Rabada, A.; Boix, E.; Thota, V.; Westcott, Z. C.; Puddu, V.; Perry, C. C. Interactions between metal oxides and

biomolecules: from fundamental understanding to applications. *Chem. Rev.* **2018**, *118* (22), 11118−11193.
(14) Zhao, X.; Nagashima, K.; Zhang, G.; Hosomi, T.; Yoshida, H.; Akihiro, Y.; Kanai, M.; Mizukami, W.; Zhu, Z.; Takahashi, T.; et al. Synthesis of monodispersedly sized ZnO nanowires from randomly sized seeds. *Nano Lett.* **2019**, *20* (1), 599−605.
(15) Yu, R.; Pan, C.; Wang, Z. L. High performance of ZnO nanowire protein sensors enhanced by the piezotronic effect. *Energy Environ. Sci.* **2013**, *6* (2), 494−499.
(16) Yasui, T.; Yanagida, T.; Ito, S.; Konakade, Y.; Takeshita, D.; Naganawa, T.; Nagashima, K.; Shimada, T.; Kaji, N.; Nakamura, Y.; et al. Unveiling massive numbers of cancer-related urinary-microRNA candidates via nanowires. *Sci. Adv.* **2017**, *3* (12), No. e1701133.
(17) Kamei, R.; Hosomi, T.; Kanao, E.; Kanai, M.; Nagashima, K.; Takahashi, T.; Zhang, G.; Yasui, T.; Terao, J.; Otsuka, K.; et al. Rational strategy for space-confined seeded growth of ZnO nanowires in meter-long microtubes. *ACS Appl. Mater. Interfaces* **2021**, *13* (14), 16812−16819.
(18) Kanao, E.; Nakano, K.; Kamei, R.; Hosomi, T.; Ishihama, Y.; Adachi, J.; Kubo, T.; Otsuka, K.; Yanagida, T. Moderate molecular recognitions on ZnO m-plane and their selective capture/release of bio-related phosphoric acids. *Nanoscale Adv.* **2022**, *4* (6), 1649−1658.
(19) Zhang, M.; Liu, T.; Du, Z.; Li, H.; Qin, W. A new integrated method for tissue extracellular vesicle enrichment and proteome profiling. *RSC Adv.* **2022**, *12* (51), 33409−33418.
(20) Wakabayashi, M.; Kyono, Y.; Sugiyama, N.; Ishihama, Y. Extended coverage of singly and multiply phosphorylated peptides from a single titanium dioxide microcolumn. *Anal. Chem.* **2015**, *87* (20), 10213−10221.
(21) Tang, J.; Yin, P.; Lu, X.; Qi, D.; Mao, Y.; Deng, C.; Yang, P.; Zhang, X. Development of mesoporous TiO2 microspheres with high specific surface area for selective enrichment of phosphopeptides by mass spectrometric analysis. *J. Chromatogr. A* **2010**, *1217* (15), 2197−2205.
(22) Kamei, R.; Hosomi, T.; Kanai, M.; Kanao, E.; Liu, J.; Takahashi, T.; Li, W.; Tanaka, W.; Nagashima, K.; Nakano, K.; et al. Rational Strategy for Space-Confined Atomic Layer Deposition. *ACS Appl. Mater. Interfaces* **2023**, *15* (19), 23931−23937.
(23) Ali, H. M.; Babar, H.; Shah, T. R.; Sajid, M. U.; Qasim, M. A.; Javed, S. Preparation techniques of TiO2 nanofluids and challenges: a review. *Appl. Sci.* **2018**, *8* (4), 587.

https://doi.org/10.1021/acsmeasuresciau.4c00089
ACS Meas. Sci. Au 2025, 5, 199−207